PROTOTYPE DESIGN OF A COMPACT POWER SUPPLY UNIT FOR REMOTE ROBOT OPERATION

Cesar G. Ferreira[1] Edson H. Watanabe[2] José Luiz S. Neto[2] Vitor F. Romano[3]
[1]Digital Dinâmica Automação Ltda.
Federal University of Rio de Janeiro [2]Electrical Engineering Dept. [3]Mechanical Engineering Dept.
watanabe@pee.coppe.ufrj.br, cesarlog@gmail.com, romano@mecanica.ufrj.br

Abstract – **One of the most challenging aspects in the design of a remote operated device located at a long distance (1 km) from its electrical power source is to provide a small and compact solution to its power supply circuitry. This article presents the concept and preliminary experimental tests performed on a compact power supply prototype, conceived to be part of the onboard hardware installed on electromechanical devices for oil & gas industry activities, such as ROVs (Remote Operated underwater Vehicles) and 2 km long pipeline inspection robots. The power supply is based on DC transmission at 1 kV, on board IGBT soft-switched inverter operating at 20 kHz, nano-technology based transformer core and rectifier to generate DC 48 V at 5 kW.**

Keywords **- DC power supply, nano-technology transformer core, DC transmission.**

I. INTRODUCTION

The use of underwater vehicles in the offshore industry activities is rapidly increasing as they can operate in deeper areas where divers cannot reach. Typical applications are: oil rigs, subsea facilities and external pipeline inspections, subsea equipments interventions and payload motion.

Onshore activities in pipelines such as internal inspection, maintenance and the elimination of clogging also requires the development of special remote operated devices. Welding and cutting of steel structures are examples of operational tasks in oil & gas sector that demand electrical power consumption in the range of few kW.

The availability of power supply at distances in the range of few km is even more critical when the need of compact units is imperative. The design of tools and devices to work inside curved pipelines of 14", 10" and 6" diameters is a technological bottleneck to be solved by mechanical and electrical engineers.

This paper presents the conceptual design and the analysis of a compact power supply, conceived to be used as part of the onboard hardware installed on electromechanical devices for oil & gas industry activities. A prototype was constructed and tests were performed to verify the feasibility of the proposed solution. The power supply is based on DC transmission at 1 kV, on board IGBT soft-switched inverter operating at 20 kHz, nanocrystaline soft magnetic based transformer core and rectifier to generate 5 kW at DC 48 V.

II. CONCEPTUAL DESIGN

The main design concept used for this distance electrical power transmission is based on the use of voltage in the range of 200V to 1 kV at the industrial frequency and the use of step-down transformer at the end of the line, so that the voltage can be reduced to acceptable nominal values at the power supply. However, using 60 Hz it is not possible to have a compact power supply. The transformer for 5 kW, 60 Hz can not be built with dimension small enough to be put inside a 6" pipeline. Even with the use of high frequency and ferrite transformer the volume of this power supply is too large for the application.

The strategy adopted here uses a 20 kHz ZVS (Zero Voltage Switching) inverter / rectifier (operating as DC/DC converter) circuitry to convert 1 kVDC to a 48 VDC source.

The transmission system is shown in Fig. 1. A transformer/rectifier stage converts the 220 VAC from the three-phase network to 1 kVDC / 5 A to be transmitted by a 2 km line. At the load end of the line, a DC/DC conversion is performed by rectifying and filtering the voltage obtained from a ZVS inverter and a high frequency transformer. This last conversion stage is located onboard, feeding the remote device with 48 VDC x 104.2 A - standard voltage to actuators such as electrical motors and hydraulic components.

The step-up transformer stage is a 60 Hz conventional three-phase transformer, since there are neither space nor weight restrictions on the source element. This is a 5 kVa transformer and weights about 55 kg.

A 20 kHz toroidal transformer made of a *Finemet* core is the main component of the DC/DC conversion stage. *Finemet* core has very small dimensions and exceptional saturation and magnetic permeability qualities [3][4]. The resultant transformer has a toroidal configuration with 85 mm external diameter and 70 mm height. An illustrative photo of the high frequency toroidal transformer and the 60 Hz conventional transformer is presented in Fig. 2, allowing for a direct comparison regarding their volumes. Both transformers have been designed for 5 kW rated power. The main characteristics of the Finemet core are: (i) high saturation magnetic flux density comparable to Fe-based amorphous metal (around 1 T) and high permeability comparable to Co-based amorphous metal; (ii) core loss about 20% of the core loss of Fe based amorphous metal and approximately the same core loss as Co-based amorphous metal; (iii) very low audio noise emission; (iv) small permeability variation (less than ±10%) at a temperature range of -50°C~150°C (v) high permeability and low core loss over wide frequency range, which is equivalent to Co-

based amorphous metal. These characteristics allow the design of a high frequency transformer much more compact than using conventional ferrite core.

The ZVS strategy is employed in order to maximize the DC/DC converter efficiency[1][2], leading to a reduction on the heat sinks dimensions.

This work will present the solutions for two important aspects concerning the DC/DC conversion: *i)* the ZVS operation independent of the load level; *ii)* a control strategy to balance the voltage and avoid the saturation of the high frequency transformer.

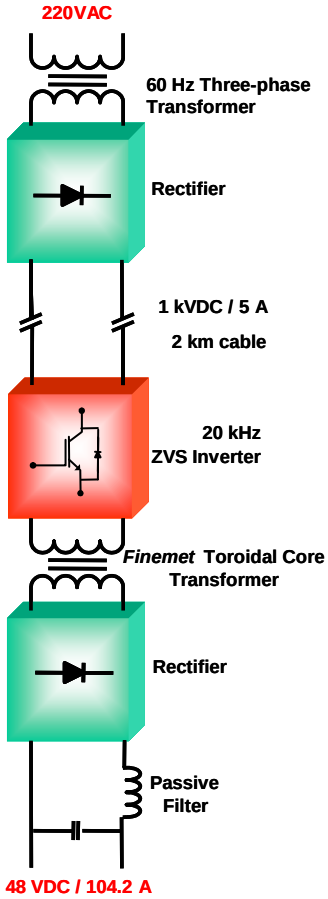

Fig. 1. Schematic representation of the transmission system and converter.

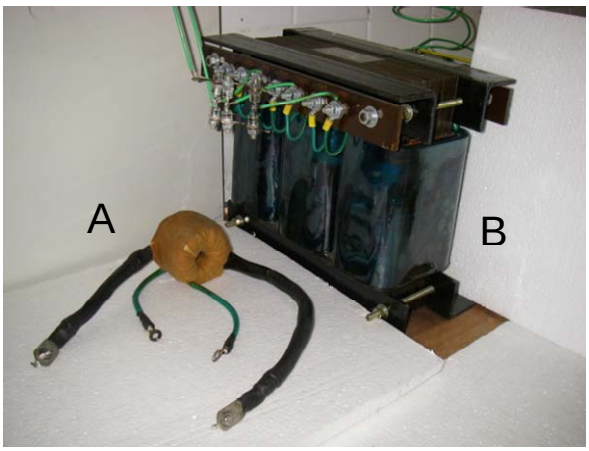

Fig. 2. Transformers: (A) 5 kW / 20 kHz toroidal Finemet and (B) three-phase / 5 kW / 60 Hz.

III. THE ZVS CONTROL

The power circuit of the 5kW ZVS inverter/rectifier is shown in Fig. 3. The inverter is composed by fast and compact 1700 V / 60 A IGBTs. When operating with conventional hard switching strategy at 20kHz and rated load, the total power loss due to each IGBT is about 200W. With ZVS mode, on the other hand, a considerable reduction in the power loss can be attained. Consequently, the heat sinks are also reduced to acceptable size.

The ZVS operation can be achieved by connecting a capacitor in parallel with each switch, as shown in Fig. 3. The voltage across the switch is, then, kept at low levels during the extinction of its current. However, the ZVS mode requires that the inverter operates at predefined load levels, since it influences the charge/discharge cycle of the capacitors.

A possible solution to this problem consists in keeping a minimum load connected at all times to the converter output. This would, obviously, implicate in more power loss. The minimum load required, however, can be purely reactive avoiding the efficiency reduction on the conversion process. The solution adopted here consists in connecting an inductor in parallel with the secondary of the toroidal transformer (Lz in Fig. 3).

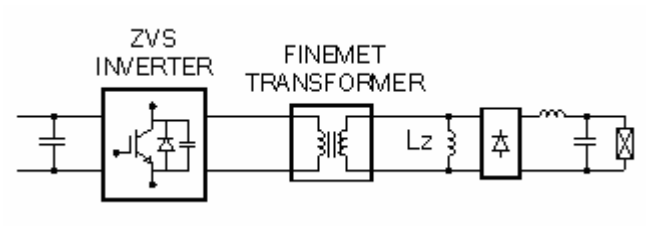

Fig. 3 – The ZVS basic power circuit.

IV. THE SATURATION CONTROL

The converter control circuit must assure that the voltage waveform at the transformer primary winding would be free from any DC component, otherwise the transformer core will saturate and the primary winding will act as a short circuit, causing possible damage to the inverter.

In order to eliminate the DC voltage component, the usual solution is to realize a feedback loop to regulate the exact time interval for each half period of the square-wave, based on the integral of the voltage across the primary winding (Fig. 4).

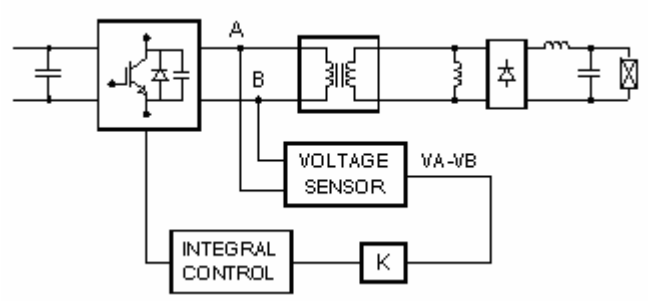

Fig. 4 - The feedback control loop using a voltage integrator.

However, the voltage integrator sensor can introduce some offset error that must be canceled. If the offset trimming is not precise enough or stable, over operational parameters variations, the saturation control will fail. The need of an accurate sensing is even more critical as higher is the working voltage.

For instance, suppose initially that there would be any DC component on the voltage across the primary winding, but consider a +1mV offset error at the input of the integrator. The closed control loop, with the integrator, will then establish an increasing negative DC voltage until an equilibrium is attained. If the feedback gain K=1, the stabilizing DC offset on the primary voltage will be −1mV.

Standard integrated analog amplifiers, however, operate with low voltage signals, usually in the range of −10V to +10V. For a 1000V at the primary, the feedback gain must be K=10V/1000V=0.01V/V, which is much less than 1. In this case, the equilibrium would be attained with a DC offset of −100mV.

The high frequency toroidal transformer used has a peak value for the magnetization current of about 150mA. Due to the volume restrictions of this project, a safety margin of 20% (30mA) of DC current component is allowed. The DC resistence of the primary winding is 0.05Ω. Therefore, the voltage drop due to the maximum tolerable DC current is 1.5mV, which is a very tiny amount if compared with 1000V.

Consequently, for this specific application, the control strategy based on the integration of the primary voltage should require extremely precise and temperature stable circuits with virtually zero offset, or a high feedback gain. As an alternative, a current integration loop could use a much larger gain (Fig. 5).

At 5kW and 1000V, the peak value of the current is 7A. The gain at the input of the integrator is 10V/7A=1.43V/A for the same signal conditioning analog circuits used.

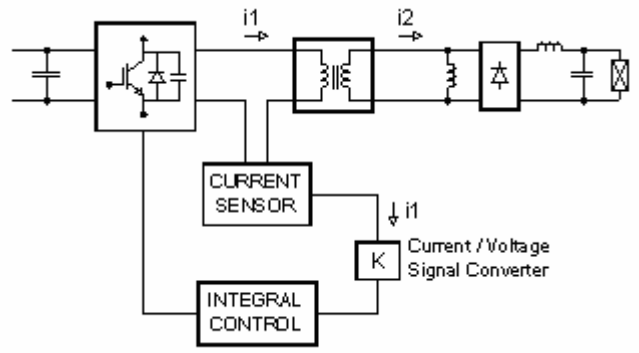

Fig. 5 - The feedback control loop using a current integrator.

A higher gain can be obtained with a circuit capable of performing the operation shown in Fig. 6, where N=16 is the turns ratio of the power transformer. One must remember that by subtracting the secondary i_2 current from the primary i_1 current, – both referred to the same winding of the transformer – equals the magnetizing i_m current, namely: Ni_1-i_2=Ni_m. A single Hall effect sensor, for instance, could be installed in order to perform this operation. Since there can't exist any DC component on i_2, the DC offset on i_1 is passed through to i_m.

It's easy to see that the output feedback gain in this case, for the maximum excursion of i_m, will be given by $N\dfrac{10V}{Ni_m}=\dfrac{16\times 10V}{16\times 0.15A}$ =66.67V/A, where the analog gain K shown in Fig. 6 is set to $\dfrac{10V}{Ni_m}=4.17V/A$, and the sensor gain is N.

A Hall effect current sensor, however, has typically a 0.001A/A output/input rapport. Thus, the analog gain should be set to K=4.17×1000=4170V/A.

Unfortunately a typical Hall sensor has an offset of about 0.2mA, which will result in 834mV of voltage offset! Nonetheless, it should be mentioned that several tests with Hall sensors were performed, along with different circuit strategies in order to cope with this shortcoming. The compensation for the Hall sensor offset, however, is not evident, for this non-ideal characteristic has hysteretic behavior. So, that rules out the use of a Hall effect current sensor in this application.

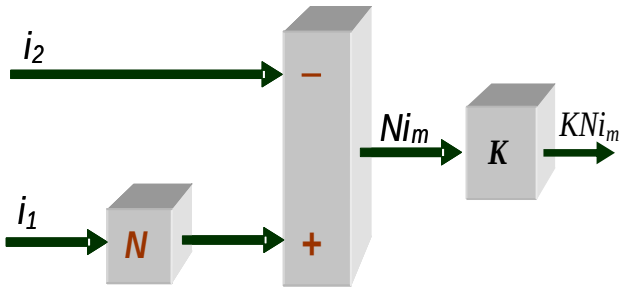

Fig. 6 – Operation that must performed in order to obtain the magnetization current.

An alternative is to use a conventional transformer to operate the current signals (transformer IMT shown in Fig. 7). Note that i_3 will carry only the AC component of i_m. However, due to the DC offset, i_m will trespass the knee point of the magnetization curve rising considerably. Fig. 8 illustrates the resultant waveform shape of i_3 for a positive offset (voltage at node **X** of the circuit on Fig. 7). By chopping this waveform symmetrically with the aid of the two zener diodes shown, the voltage at node **Y** will have an offset with the same polarity as the DC component on i_m. This signal can then be integrated, and the closed control loop reaches stability canceling the DC offset, as proven by the results presented by Fig. 9 and Fig. 10.

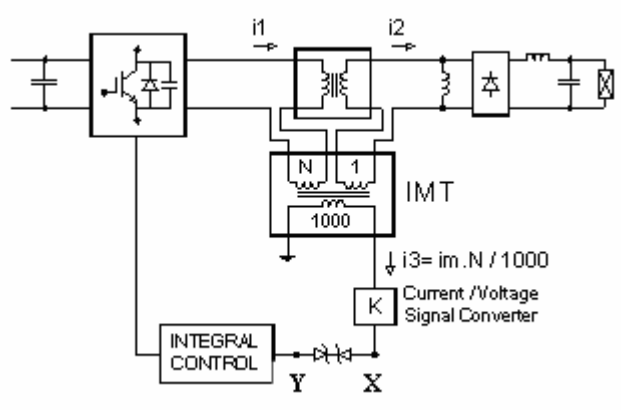

Fig. 7 - The feedback control loop by integrating i_m.

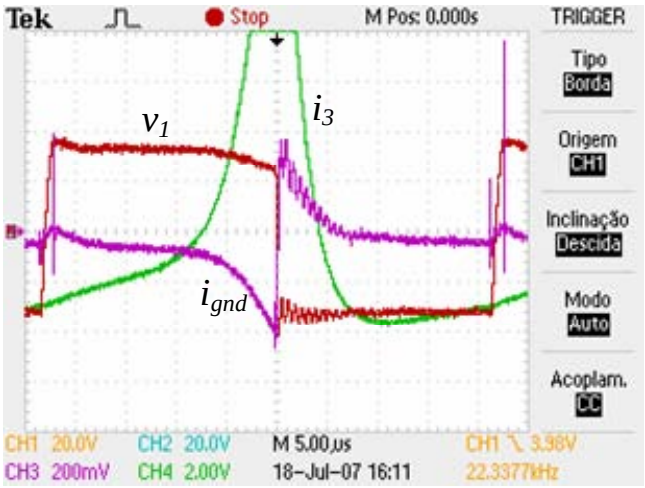

Fig. 8 – Experimental results on open loop (V_{DC}=30V): v_1=CH1-CH2 (V); Ni_m=CH4 (A); $i$gnd=CH3(A/4).

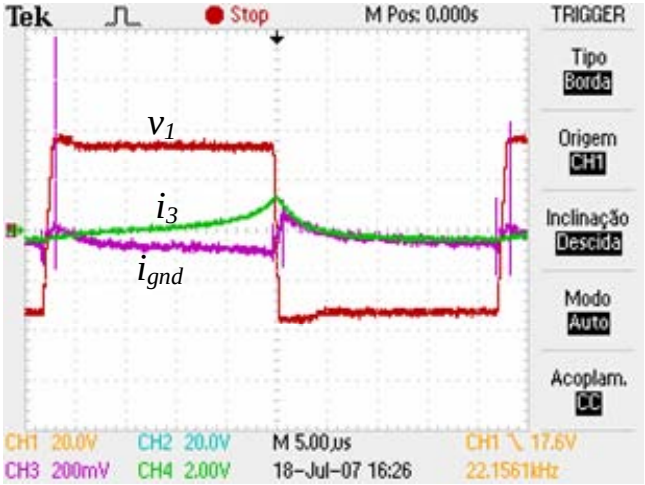

Fig. 9 – Experimental results on closed loop control (V_{DC}=30V): v_1=CH1-CH2 (V); Ni_m=CH4 (A); $i$gnd=CH3(A/4).

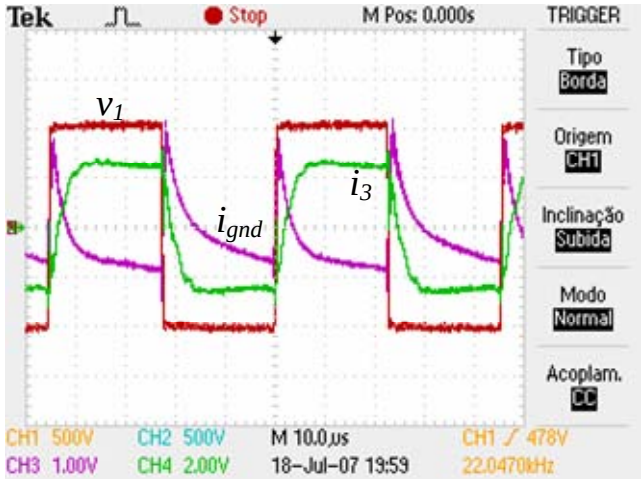

Fig. 10 – Experimental results on closed loop control (V_{DC}=1000V): v_1=CH1-CH2 (V); Ni_m=CH4 (A); $i$gnd=CH3(A/4).

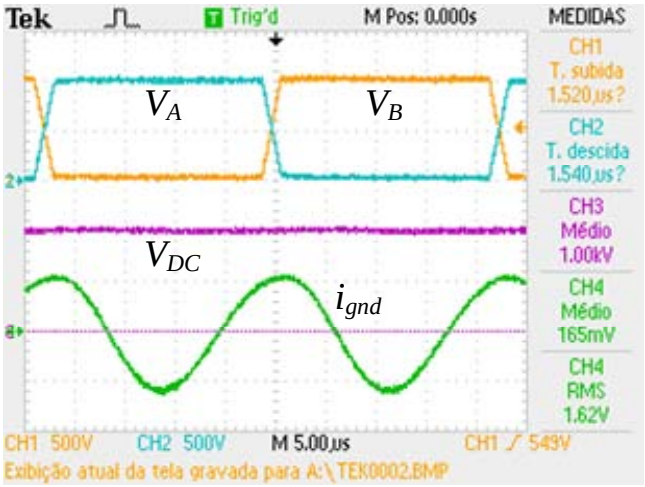

Fig. 11 - Experimental results (V_{DC}=1000V) with no load.

V. EXPERIMENTAL RESULTS

The strategy explained in the previous section was applied to a laboratory prototype. The ZVS inverter synthesizes a square-wave voltage of 20kHz. Fig. 10 and Fig.11 present the ZVS operation at 1000V for full load and no load respectively. As one can see the ZVS control is effective and not depends on the load level.

VI. CONCLUSION

This article presented the concept and preliminary experimental tests performed on a compact power supply prototype, conceived to be part of the onboard hardware installed on ROVs, located at the end of a 2km.

The solutions for two important aspects concerning the DC/DC conversion were presented: *i)* the ZVS operation independent of the load level; *ii)* a control strategy to balance the voltage and avoid the saturation of the high frequency transformer.

ACKNOWLEDGEMENTS

This project was supported mainly by CT-Petro/CNPq and partially by FAPERJ.

REFERENCES

[1] Jovanovic, M.M.; Tabisz, W.A.; Lee, F.C., "Zero-voltage-switching technique in high-frequency off-lineconverters", Applied Power Electronics Conference and Exposition, 1988. APEC 88, Conference Proceedings 1988., 1-5 Feb 1988 Page(s):23-32.

[2] Nederson do Prado, R. "The behavior of ZVS converters with a nonlinear resonant inductor" , Industrial Electronics, Control, and Instrumentation, 1995., Proceedings of the 1995 IEEE IECON, Volume 1, 6-10 Nov. 1995 Page(s):341 – 346.

[3] Fukunaga, H.; Eguchi, T.; Koga, K.; Ohta, Y.; Kakehashi, H. "High performance cut cores prepared from crystallized Fe-based amorphous ribbon", IEEE Transactions on Magnetics, Volume 26, Issue 5, Sep 1990 Page(s):2008 – 2010.

[4] Hitachi Metals, "Nanocrystaline soft magnetic material - FINEMET", Product Catalog, , 2004 http://www.hitachi-metals.co.jp/e/prod/prod02/p02_22.html.